

A possible way of understanding the differential motion of minor ions in the solar wind

C.-Y. Tu

Department of Geophysics, Center for Space Science, Peking University and Laboratory of Space Weather, Chinese Academy of Sciences, Beijing, China

L.-H. Wang

Department of Physics and Space Science Laboratory, University of California, Berkeley, California, USA

E. Marsch

Max-Planck-Institut für Aeronomie, Katlenburg-Lindau, Germany

Received 26 June 2002; revised 16 December 2002; accepted 29 January 2003; published 22 April 2003.

[1] Measurements with Solar and Heliospheric Observatory (SOHO)/Charge, Element, and Isotope Analysis System (CELIAS) in high-speed solar wind show that some minor ions such as O^{6+} have a relatively high drift velocity; however, other ions such as Fe^{9+} tend to lag behind oxygen by a few tens of km/s [Hefi *et al.*, 1998]. This subtle observational feature has not yet been understood. A possible way, based on the quasi-linear theory of cyclotron resonance, of understanding this phenomenon is presented in this paper. The charge per mass of the ion O^{6+} and Fe^{9+} are different, a fact which results in different features of the ion-cyclotron resonance with waves. In plasma with protons, drifting alpha particles, and electrons, the dispersion relation of cyclotron waves has two branches. The oxygen ions tend to resonate with the inward propagating waves of the left-hand-polarized (LHP) first branch and the outward propagating waves of the LHP second branch. These resonances may together lead to a velocity distribution with a central velocity higher than the proton (solar wind) bulk velocity by about 50 km/s at 1 AU. The Fe^{9+} ions tend to resonate with both the inward and outward propagating waves of the first branch and may thus form a velocity distribution with a central velocity very near the proton bulk velocity. These analytical results are shown to be supported by numerical results from a two-dimensional simulation based on the quasi-linear diffusion equation. The limitations of the present analysis and further work, which should be done to support the ideas proposed here, are also discussed. **INDEX TERMS:** 2164 Interplanetary Physics: Solar wind plasma; 2159 Interplanetary Physics: Plasma waves and turbulence; 7867 Space Plasma Physics: Wave/particle interactions; 7871 Space Plasma Physics: Waves and instabilities; **KEYWORDS:** solar wind ions, ion differential streaming, pitch angle diffusion, ion-drift regulation

Citation: Tu, C.-Y., L.-H. Wang, and E. Marsch, A possible way of understanding the differential motion of minor ions in the solar wind, *J. Geophys. Res.*, 108(A4), 1161, doi:10.1029/2002JA009561, 2003.

1. Introduction

[2] Hefi *et al.* [1998] showed with Solar and Heliospheric Observatory (SOHO)/Charge, Element, and Isotope Analysis System (CELIAS) data that O^{6+} ions have usually a higher bulk speed than protons, similar to what was observed before for $^4He^{2+}$ [Marsch *et al.*, 1982b]. They also showed the new phenomena that silicon Si^{7+} and iron Fe^{9+} tend to lag somewhat behind oxygen by 25 km/s, while O^{6+} ions have velocities of about 635 km/s, and protons have a main velocity near 600 km/s (see their Figure 4). If one considers the angle between the magnetic field and the radial direction of about 45° at 1 AU, the O^{6+} ions may even

have a mean drift velocity as large as 52 km/s along the magnetic field line. This result is consistent with a previous observation with ICI/ISEE-3; see data by Bochsler [1989]. He found that in high-speed solar wind silicon ions lag by about 20 km/s behind $^4He^{2+}$. Schmid *et al.* [1987] also found at the upper end of their observed velocity range (at about 500 km/s) a tendency for iron ions to lag behind $^4He^{2+}$ by about 20 km/s. Neugebauer [2001] quoted all these observations of ion differential motions. We believe these observations are reliable and represent real phenomena in the solar wind.

[3] However, these observations are difficult to understand from previous theories. Considerable effort has been made in the last twenty years to understand the mechanism generating the drift velocities of solar wind minor ions [Marsch *et al.*, 1982c; Isenberg and Hollweg, 1983; Isen-

berg, 1984; Marsch, 1999; Hu, 2000]. In all these models the acceleration was calculated while considering only resonances of the ions with the first branch of ion-cyclotron waves and assuming a power law wave spectrum. Diffusion in velocity space was also not considered in these models. The acceleration rate of ions was found [Isenberg and Hollweg, 1983; Hollweg, 1999a, 1999b, 1999c] to be inversely proportional to the ratio of charge per mass, if the slope of the power spectrum is steeper than -2 . For the acceleration of oxygen ions Isenberg and Hollweg [1983] even assumed a power index of -3 and found that the model resulted in an oxygen differential velocity of about the Alfvén speed, and that the iron ions are clearly faster than oxygen. These results are consistent with recent results by Hu *et al.* [2000], who showed that O^{5+} ions were more strongly accelerated than $^4He^{2+}$ ions.

[4] However, Fe^{9+} ions have a charge-per-mass number of 0.16, while for O^{6+} this number is 0.38. So according to these models, iron ions should be much more accelerated than oxygen ions. However, the differential ion velocity predicted by these models is opposite to the trend actually measured by CELIAS on SOHO [Hefti *et al.*, 1988]. This failure in explaining the observations may perhaps not come from the quasi-linear theory of cyclotron resonance itself, but from the assumptions made previously, such as considering only the first-branch outward propagating waves and assuming a bi-Maxwellian velocity distribution.

[5] Gomberoff and Elgueta [1991], Gomberoff *et al.* [1996a, 1996b], and Gomberoff and Astudillo [1999] suggested that, in a multicomponent plasma such as the solar wind, the left-polarized cyclotron waves heat and accelerate first those ions having the smallest charge-per-mass number. When these ions have been accelerated, their drift motion changes the topology of the dispersion relation, and this opens a new channel to heat and accelerate further the ions with the next smaller charge-per-mass number. This model predicts the highest drift velocity for ions with the smallest charge-per-mass number. Therefore, it cannot explain why the observed Fe^{9+} ions got a smaller drift velocity than the O^{6+} ions.

[6] Giving up the model restrictions of fixed wave spectra and rigid velocity distributions, several authors [Tam and Chang, 1999, 2001; Isenberg, 2001a; Ofman *et al.*, 2001; Isenberg *et al.*, 2000, 2001; Tu and Marsch, 2001a, 2001b; Marsch and Tu, 2001; Tu and Marsch, 2002; Cranmer, 2001; Vocks and Marsch, 2002; Tu *et al.*, 2002] have recently applied successfully the cyclotron-resonance diffusion theory to explain the regulation of the proton beam and temperature in the solar wind and the shapes of proton and minor ion velocity distribution functions. The velocity-space diffusion, of plasma ions in resonance with cyclotron waves that propagate parallel to a background magnetic field, has in the past been studied in considerable detail [e.g., Shapiro and Shevchenko, 1962; Kennel and Engelmann, 1966; Rowlands *et al.*, 1966; Skilling, 1971; Davidson, 1972]. Gendrin [1968] and Gendrin and Roux [1980] also presented the diffusion curves corresponding to He^+ ions in the magnetosphere, interacting with both left-hand and right-hand-polarized waves. Hollweg [1999a, 1999b, 1999c, 2000] assumed in his solar wind models a finite wave power for both the first and second branch wave modes.

[7] Here we suggest that the differential velocities of oxygen and iron ions may be due to the fact that these two kinds of ions are in resonance with various wave modes obeying, respectively, different branches of the dispersion relation as determined for a plasma consisting of protons, drifting alpha particles and electrons. Following this idea, the observations can be qualitatively explained by considering the relevant diffusion plateaus. This explanation is supported by results from a two-dimensional numerical simulation, which is based on the quasi-linear diffusion equation.

2. Dispersion Relations

[8] The well known quasi-linear theory was for our present purpose already described in detail by Cranmer [2001] and Tu *et al.* [2002]. They developed a two-dimensional numerical code for solving the quasi-linear diffusion equation. We will therefore not duplicate these results here, but only give a very simple description. The dispersion relation in a plasma with protons, drifting alpha particles and electrons may be written as follows [Stix, 1992; Tu and Marsch, 2001a]

$$y^2 = \frac{x^2}{1 \mp x} + \frac{4\eta_\alpha(x - yU_\alpha)^2}{1 \mp 2(x - yU_\alpha)} \quad (1)$$

where $x = \omega(k_{\parallel})/\Omega_p$, $y = (k_{\parallel}V_A)/\Omega_p$, the abundance $\eta_\alpha = 0.05$, and in units of V_A the drift speed of the alpha particles $U_\alpha = 0.8$. The ion gyrofrequency is $\Omega_i = q_i B_0/(m_i c)$, with the index $i = p$ for protons. Here q_i is the charge of ion species i , m_i its mass, and B_0 the background magnetic field. As usually, c denotes the speed of light. The abbreviation LHP stands for left-hand polarization and RHP for right-hand polarization. The minus sign in (1) refers to LHP and the plus to RHP.

[9] The solution of this equation is shown in Figure 1. The left-hand part of the figure shows four LHP branches. The thin dash-dot-dash line is the first branch, which is denoted by LO-1, with outward propagation sense. The dash-dot-dot-dash line shows the second branch, which is denoted by LO-2, with outward propagation sense. The thin solid line shows the first branch, which is called LI-1, with inward sense of propagation. The thick dash-dot-dash line shows the second branch, which is called LI-2, with inward propagation sense. In the right-hand figure the dotted line shows the first RHP branch with outward propagation sense, which is designated by RO-1. The dashed line shows the second RHP branch with outward propagation sense, which is designated by RO-2. The first branches may be considered as being related to the dispersion relation as determined by a proton-electron plasma, yet they are severely influenced by the drifting alpha particles.

[10] It should be pointed out that the curves shown in Figure 1 are the mathematical solutions of equation (1). Presently, we have no observational evidence for the existence in the solar wind of waves obeying these dispersion relations. In particular, the damping rates of the RO-2 and LO-2 waves may be high, because these waves are close to the helium resonance. However, if a plateau in the helium velocity distribution is formed by diffusion, then damping

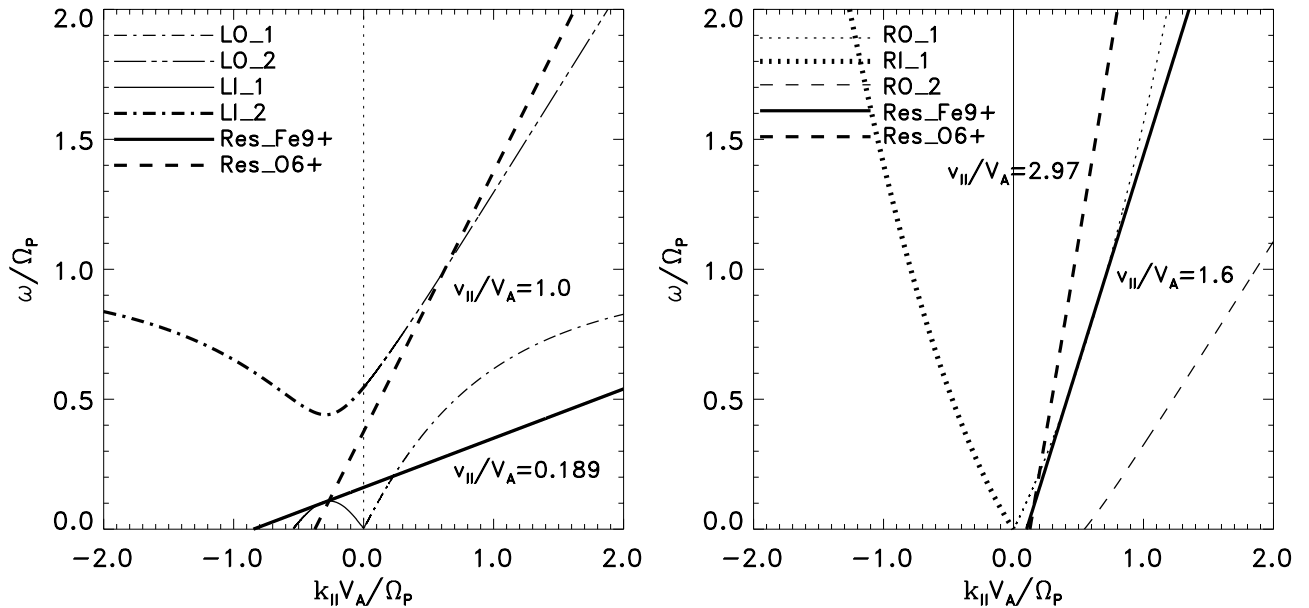


Figure 1. The dispersion relation of a cold plasma consisting of electrons, protons, and alpha particles, with abundance $\eta_\alpha = 0.05$ and drift speed $U_\alpha = 0.8$. The legend for the various wave dispersion branches is also given in the upper left corner. The left panel shows the dispersion relation of LHP waves: The thin dash-dot-dash line refers to outward first-branch waves, dash-dot-dot-dash outward second-branch, thin solid inward first-branch, and thick dash-dot inward second-branch. The right panel gives the dispersion relation of RHP waves. The thin dotted line refers to outward first-branch waves, the dashed to outward second-branch, and the thick dotted to inward first-branch waves. In both panels, the thick solid lines show examples of the resonance condition of Fe^{9+} ions, the thick dashed lines show an example of the resonance condition for O^{6+} ions. The corresponding parallel velocities are given at the respective curves.

will cease or be small, and the excitation of these wave modes becomes possible. We will not discuss this process in detail, but we will just assume here that waves with the dispersion relation (1) exist and discuss the resulting diffusion and plateau in the velocity distribution of the Fe^{9+} and O^{6+} ions.

[11] As the first step to explore the potential of this new idea for understanding the minor ion differential speeds in the solar wind, we use in our analysis the cold plasma dispersion relation, an assumption which is still widely used in solar wind model calculations [e.g., *Hollweg, 2000*] and even in simulations of the evolution of the velocity distributions of the solar wind ions [e.g., *Tam and Chang, 1999*], which are known to be at high temperature. Yet, in principle, finite temperature effects and the thermal anisotropy play an important role in the dispersion relation. Thermal effects on the ion diffusion are certainly important but complicated. In the literature, the dispersion relation of the thermal solar wind plasma has mostly been calculated assuming a drifting bi-Maxwellian velocity distribution. However, this assumption must be given up in a serious, i.e. self-consistent, treatment of diffusion in velocity space. Probably, a full particle simulation may help to solve this problem.

[12] In Figure 2 the dispersion relation for a warm plasma with a drifting bi-Maxwellian velocity distribution is presented. This dispersion is obtained from a numerical solution of the equations presented in text books [e.g., *Stix, 1992, p. 267*]. Here $\beta_{p||} = 0.3$ and the anisotropy $A_p = 1.5$, which are

typical values for the near-Sun solar wind. For He^{2+} we take $T_{\alpha||} = 3T_{p||}$, $A_\alpha = 0$ and $U_\alpha = 0.8 V_A$, all parameters having values observed usually in the fast solar wind [*Marsch et al., 1982a, 1982b*]. We see that the topology of the dispersion curves does not change a lot as compared with the cold plasma dispersion. The growth of LI-2 and LO-1 wave modes results from the small thermal anisotropy we assumed for the protons. The damping rates are very small for these two modes, but for the LO-2 mode the damping is strong. However, if we consider that the velocity distribution of the alpha particles may form a plateau, the damping caused by them may fade away. Then the LO-2 waves can exist and be generated by the sizable anisotropy of the bi-Maxwellian proton core distribution (see, e.g., equation (A14) of *Tu and Marsch [2001a]*). This is just a possibility. In fact, we do not know how the dispersion relation will actually change in response to resonance diffusion. Of course, a self-consistent study is needed to settle this open issue.

[13] The thick straight lines in the left-hand and right-hand panels show the resonant conditions for the iron ion Fe^{9+} with RHP and LHP waves, respectively. This condition reads:

$$\frac{v_{||}}{V_A} = \frac{x}{y} \mp \frac{\Omega_i}{\Omega_p} \frac{1}{y} \quad (2)$$

We see from this relation and Figure 1 that the iron ion Fe^{9+} can resonate with both inward and outward waves of the

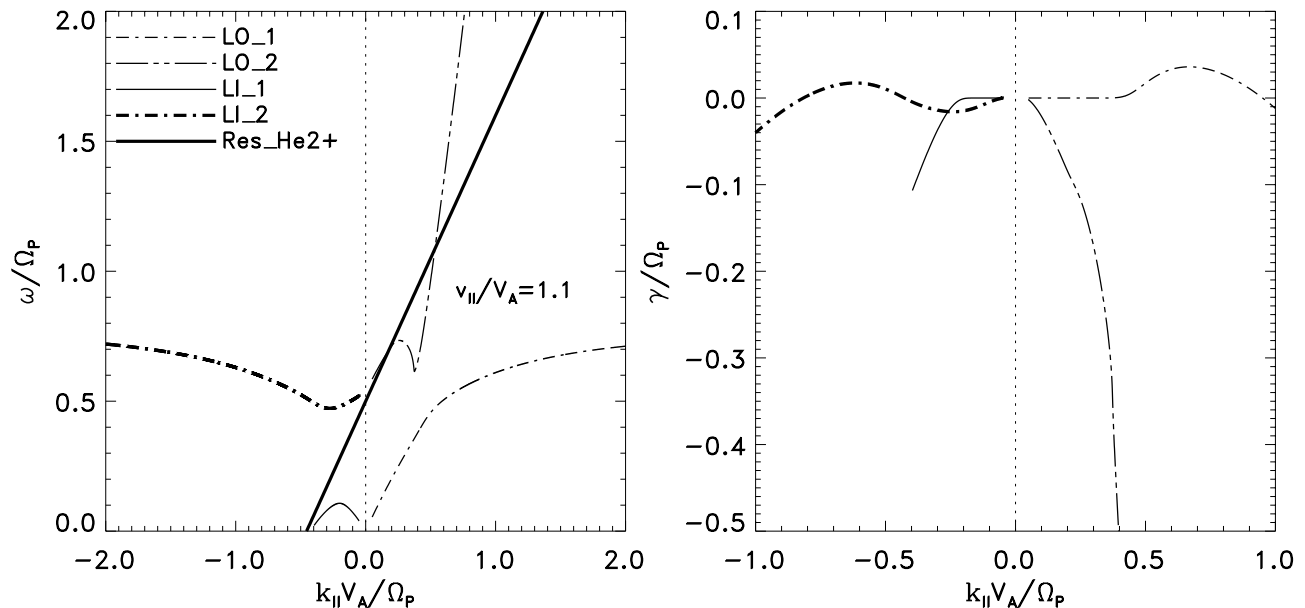


Figure 2. This figure shows the dispersion relation (left panel) and damping rate (right panel) of LHP waves in a thermal plasma with $A_p = 1.5$, $\beta_{p||} = 0.3$, $\eta_\alpha = 0.05$, $A_\alpha = 0$, $T_{\alpha||} = 3 T_{p||}$, $U_\alpha = 0.8$, $T_e = T_{p||}$ and $A_e = 0$. The electron density and drift are calculated by consideration of the zero-current condition and charge-neutrality condition. The thick solid line shows the resonance condition of alpha particles with speed: $v_{||} = 1.1 V_A$. The legend for the various wave dispersion branches is as in Figure 1 and also given in the upper corner of the left panel.

first branch at small wave numbers and frequencies. The resulting resonant diffusion may therefore yield a velocity distribution with a small positive bulk velocity.

3. Diffusion of Iron Ions

[14] If the waves on these branches are strong enough, the quasi-linear diffusion will lead to a time asymptotic state with a diffusion plateau [Isenberg and Lee, 1996; Marsch and Tu, 2001]. Diffusion plateaus are defined by vanishing pitch angle gradients on circular isodensity contours in velocity phase space with respect to a coordinate system moving with the phase speed of the waves. The bottom panel of Figure 3 shows examples of such contours, referring to the wave modes, LO-1, LI-1, RO-1, LO-2, LI-2 and RO-2, respectively, with the same line style as used in Figure 1. In the calculations presented in this report, V_A is chosen as 30 km/s and $\Omega_p = 0.397$ rad/s, parameters corresponding to the situation near 1 AU. The wave numbers that correspond to each of the resonant contours in the bottom panel of Figure 3 are plotted versus particle parallel speed in the middle panel, and the related wave phase velocity in the upper panel.

[15] We see from the bottom panel of Figure 3 that the plateau contours, which are formed from the particle resonances with the waves of branches LO-1 and LI-1, cross each other at the parallel velocity near 10 km/s. The diffusion driven by resonance with LO-1 and LI-1 waves may help to form a velocity distribution with small bulk velocity. The diffusion caused by resonance with waves of the branch LI-1 may prevent the ions from any further acceleration. The bottom panel shows that LO-2 wave and RO-1 waves can also support a separate velocity distribu-

tion. However, the deceleration by LI-1 waves may prevent Fe^{9+} from achieving a high parallel speed.

[16] Figure 4 shows the time evolution of the Fe^{9+} velocity distribution simulated from the 2-D code, which was developed by Tu *et al.* [2002, 2003] for solving the time-dependent quasi-linear diffusion equation. In this calculation only the wave modes LO-1 and LI-1 are considered. The initial velocity distribution was assumed to be a Maxwellian distribution with $w_{||} = w_{\perp} = 44$ km/s and $u_{||} = 10$ km/s, where $w_{||}$ is the parallel and w_{\perp} the perpendicular thermal speed, and $u_{||}$ is the parallel component of the bulk velocity. The computational grid spanned in $v_{||}$ from -159 km/s to 181 km/s, and in v_{\perp} from 0 km/s to 201 km/s, with a grid size of 2 km/s for both velocity components. The boundary conditions were: a constant extrapolation of the velocity distribution at $v_{\perp} = 0$ and quadratic extrapolation in the integration variable along the other three edges of the numerical grid in velocity space [see, e.g., Cranmer, 2001].

[17] The Lax-Wendroff scheme and simple FTCS (forward-time-centered-space) scheme are used for the first-order and second-order derivatives, respectively. For simplicity, we assume in the simulation that no Fe^{9+} ions resonate simultaneously with both wave modes, so that their velocity space is divided into two regions, I and II, corresponding to the respective values of $v_{||}$. We will discuss the limitations of this assumption later. In region I, the Fe^{9+} ions are in resonance with the outward first-branch LHP waves and in region II with the inward first-branch LHP waves. At the boundary between regions I and II, we assume [see Tu *et al.*, 2002, 2003] that the phase-space density is determined by the parallel diffusion flux, which is evaluated by help of the conservation equation for the

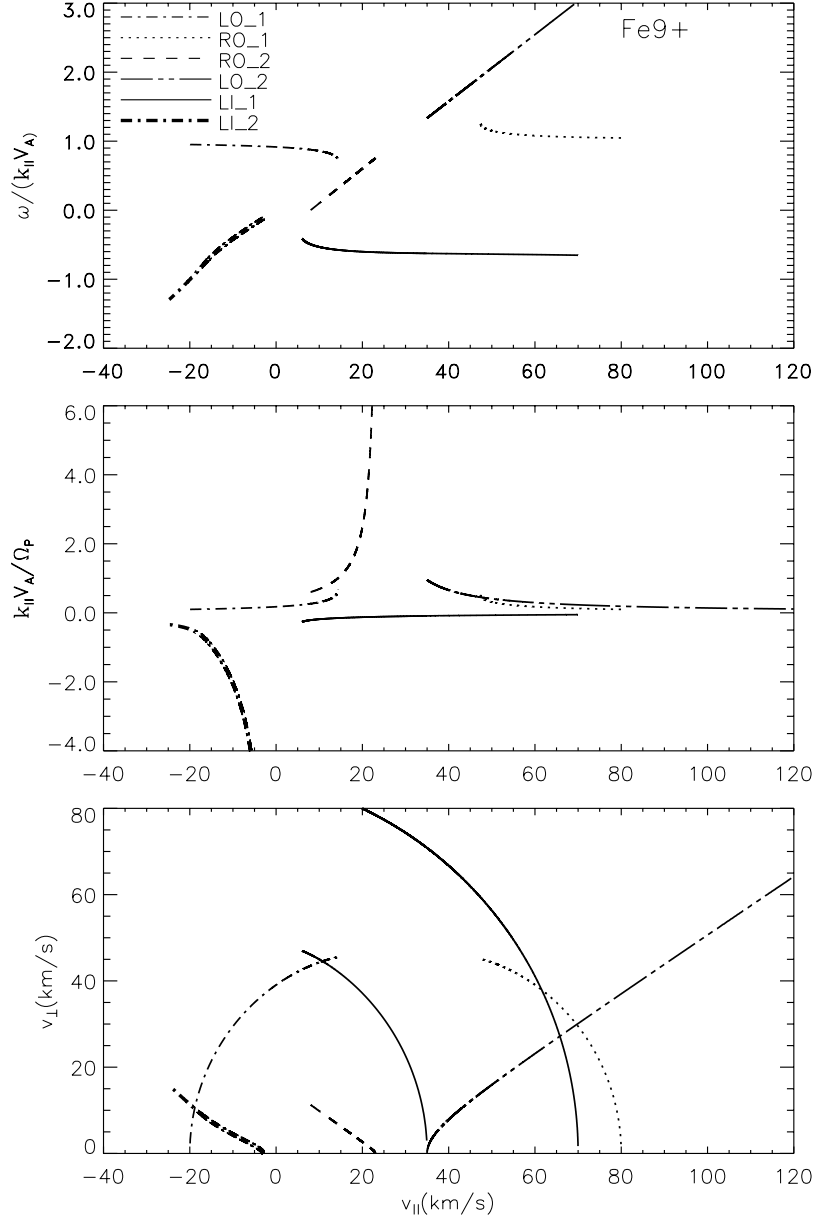


Figure 3. The curves in the bottom panel delineate examples of plateau contours for the Fe^{9+} ions, which are calculated from the diffusion-plateau condition and determined by the resonance with, from left to right, the outward first-branch LHP, inward second-branch LHP, outward second-branch RHP, inward first-branch LHP, outward second-branch LHP and finally outward first-branch RHP waves. The greatest resonant v_{\parallel} for the LO-1 branch is 14.4 km/s and the lowest for LI-1 is 6.02 km/s. Ions with v_{\parallel} between these two values will be in resonance with both wave modes. The lowest v_{\parallel} for the RO-1 branch is 47.4 km/s, for the RO-2 branch 8 km/s. The largest v_{\parallel} is about $0.8 V_A$. The lowest v_{\parallel} for the LI-2 branch is -24.7 km/s. The lowest v_{\parallel} for the LO-2 branch is about $0.8 V_A$. The middle panel shows the corresponding normalized wave number, y , as a function of v_{\parallel} , and the upper panel shows the normalized phase velocity.

phase-space density. We take a wave-energy spectrum having a power law form:

$$P_B(k_{\parallel}) = P_0 \left(\frac{|k_{\parallel}|}{k_0} \right)^{-\eta} \quad (3)$$

where, for the outward first-branch LHP waves, the spectral index is $\eta = 5/3$, and the reference wave vector

$k_0 = 10^{-10}/\text{cm}$ and power $P_0 = 1.36 \times 10^1 \text{ G}^2 \text{ cm}$. For the inward first-branch LHP waves, $\eta = 5/3$ and $k_0 = 10^{-10}/\text{cm}$ and $P_0 = 1.36 \times 10^{-1} \text{ G}^2 \text{ cm}$. The time step was chosen to be 10^{-5} s. The program conserves the particle number well, since it may run for a million time steps, with the particle density varying by less than three in one thousand. We see in the bottom panel of Figure 4 the final stable velocity distribution. The pertinent bulk velocity is: $u_{\parallel} = 7.5$ km/s,

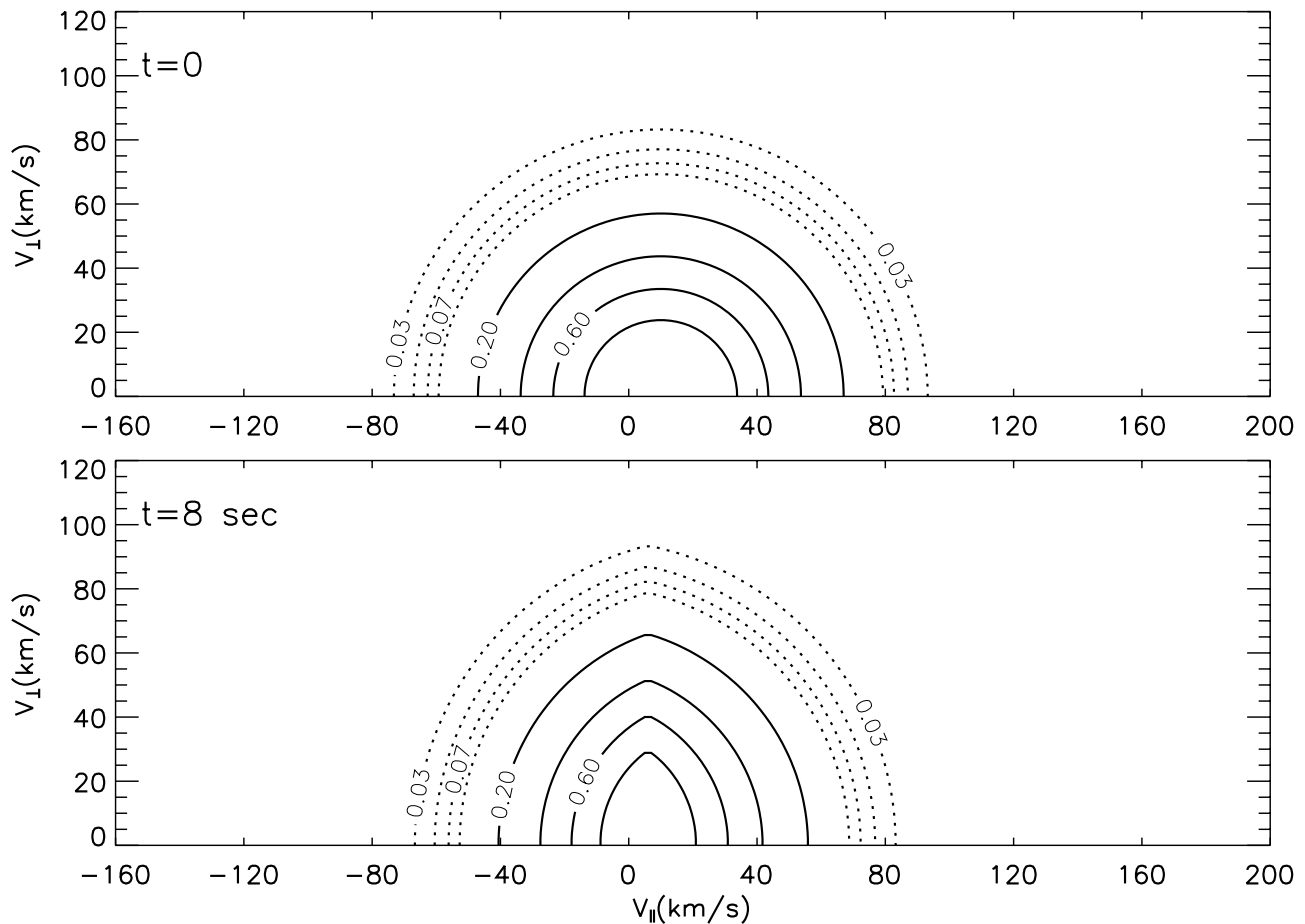


Figure 4. Evolution of the velocity distribution of Fe^{9+} ions. Upper panel shows the initially assumed Maxwellian distribution with $w_{\parallel} = w_{\perp} = 44$ km/s and $u_{\parallel} = 10$ km/s. The bottom panel shows the simulation results after 800001 time steps in the numerical calculation. A time step is 10^{-5} s.

the anisotropy, $A = (T_{\perp}/T_{\parallel} - 1)$, is 0.6. The parallel and perpendicular thermal velocities are, respectively, 38.5 km/s and 48.6 km/s.

[18] We now recapitulate briefly the assumptions made in the simulation. When we calculated the diffusion plateaus shown in the bottom panel of Figure 3, we assumed that enough wave energy exists on each dispersion branch, extending without limitation all the way to $k_{\parallel} = 0$, as shown in Figure 1. The segments in the middle and upper panel of Figure 3 are determined, respectively, from the corresponding diffusion-plateau contours. Figure 4 shows that, if the waves on these two branches are intense enough, the waves of the LI-1 and LO1 branches can together support a stable velocity distribution of the Fe^{9+} ions. The whole wave energy spectrum (not only segments) is assumed to be described by equation (3). The amplitude of outward waves is consistent with the observations by *Denskat and Neubauer* [1982]. The amplitude of inward waves is arbitrarily assumed, with the idea that inward waves should be much weaker than outward ones. The final, stable distribution shown in Figure 4 does not depend on the wave amplitude and spectrum slope we assumed.

[19] However, in the simulation we assumed that in each velocity space region, I or II, the ions are resonant with only one wave mode. From Figures 1 and 3 we see that

the Fe^{9+} ions cannot resonate simultaneously with both LI-1 and LO-1 modes in most of the v_{\parallel} range, except for the small velocity range from 6 to 14.4 km/s, delimited by the thick line and the line (not shown in the figure) which is tangential to the curve LO-1 and goes through the points $x = 0.16$ and $y = 0$. In this velocity range the ions can resonate with both wave mode simultaneously. *Isenberg* [2001b] suggested that the resonance with both inward- and outward-propagating waves will necessarily produce preferential heating of heavy ions, like in second-order Fermi acceleration. The ions may change between contours with different kinetic energy as evaluated in the wave frame for this velocity region. This is an important physical process for the formation and evolution of the ion velocity distribution and should be studied in the future work.

[20] The purpose of the present simulation was to show that a stable Fe^{9+} ion velocity distribution with low bulk drift velocity may be supported by interaction with both the LI-1 and LO-1 mode. So we did not include the cross-contour diffusion in our present simulation. Furthermore, it is not easy to study this mechanism, because the energy diffusion depends on the detailed spectrum of both type of waves, which we do not know anyway. It will also require a much more complicated numerical code in order to deal

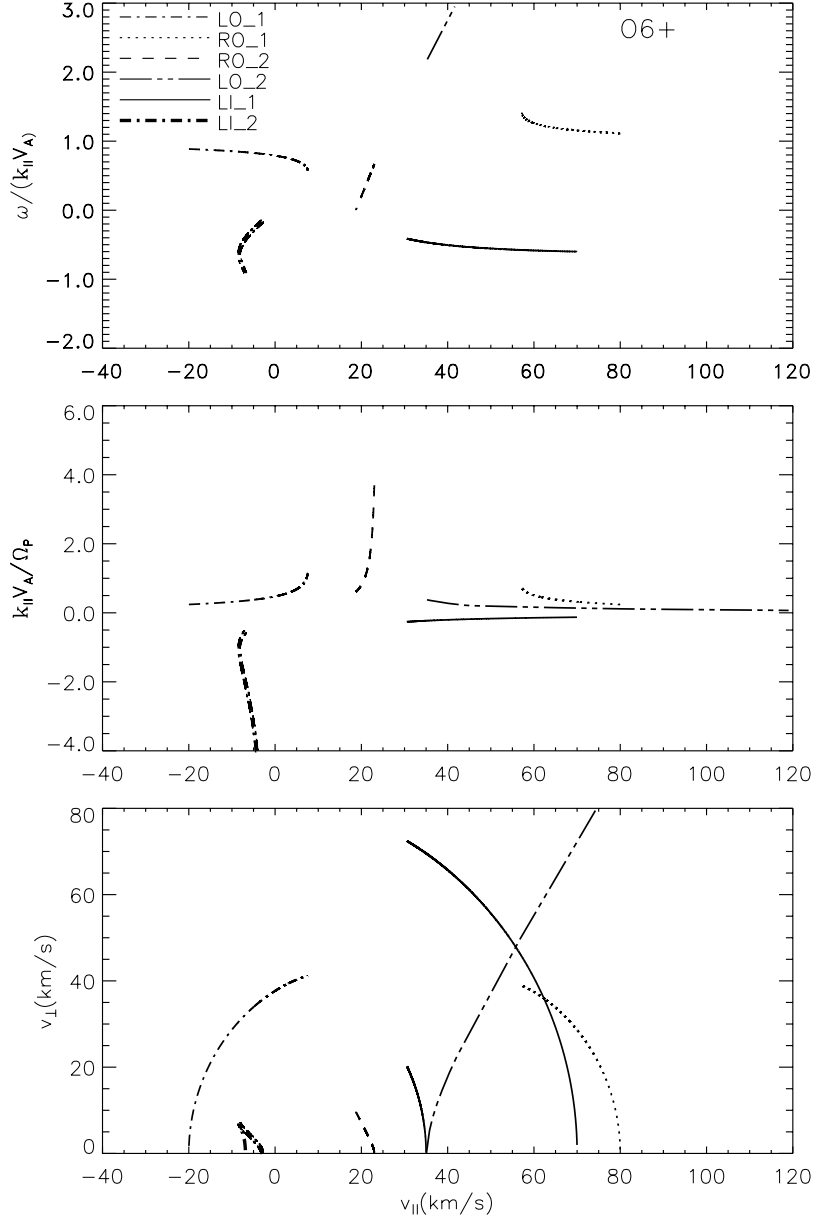


Figure 5. Same format as in Figure 3, but for oxygen ions, and same scaling for v_{\parallel} . The largest v_{\parallel} for the LO-1 branch is 7.57 km/s and for the LI-2 branch -4.8 km/s. The lowest v_{\parallel} for the LI-2 branch is -8.33 km/s. The lowest v_{\parallel} for the RO-2 branch is 18.7 km/s and the highest is about $0.8 V_A$. The lowest v_{\parallel} for the LI-1 branch is 30.6 km/s and for the RO-1 branch 57.2 km/s. The lowest v_{\parallel} for resonance with the LO-2 branch is about $0.8 V_A$.

simultaneously with the diffusion caused by the two wave modes.

4. Diffusion of Oxygen Ions

[21] We now discuss the formation of the velocity distribution of oxygen ions by cyclotron resonant diffusion. In Figure 1, the dashed thick lines represent the resonance conditions of the oxygen ion O^{6+} . We see that the ions can resonate with six wave modes, in principle. Examples of the diffusion plateaus related to each wave mode are shown in Figure 5, which has the same format as Figure 3. To ease the comparison of both figures, the v_{\parallel} -values of the intersection

points of the plateau contours with the v_{\parallel} -axes in Figures 3 and 5 are the same, respectively. We can see that the resonances with LO-2 and LI-1 waves can support a stable velocity distribution. The oxygen ions with small velocities cannot resonate with LI-1 waves. However, the oxygen ions with velocity greater than 30.6 km/s can resonate with both LI-1 waves and LO-2 waves. If we assume that during the resonance v_{\perp} increases, then we can conclude that resonance with LI-1 waves results in ion deceleration in the parallel direction, while resonance with LO-2 results in ion acceleration.

[22] The differences observed in the drift velocities of the Fe^{9+} and O^{6+} ions can be understood as resulting from their

different gyro frequencies. The normalized gyro frequency, $\Omega_{\text{Fe}^{9+}}/\Omega_p$, is very small and equals $9/56 = 0.16$, and thus the resonance line through the point $(0, 0.16)$ crosses the inward as well as outward first dispersion branch. However, for O^{6+} ions, the resonance line goes across the point $(0, 0.375)$, which is higher up on the vertical axis, and thus it cannot intersect both first branches simultaneously. This difference causes different behaviour in the diffusion, as is shown in Figures 3 and 5.

[23] From Figure 3 we can see that for the Fe^{9+} ions the two curves intersect, which delineate the location of the plateau as determined by LI-1 and LO-1 waves, respectively. Therefore, closed isodensity contours in velocity phase space may be formed by diffusion. Figure 4 shows that a stable velocity distribution can be supported by these two wave modes. However, we infer from Figure 5 that for O^{6+} the two plateau curves do not meet. There is a gap for v_{\parallel} ranging from 7.57 km/s to 30.6 km/s. So, these two wave modes cannot support a stable velocity distribution.

[24] From Figures 1 and 5 we can see that resonance with RO-2 waves may only take place for ions in a very small velocity range. Thus, the resonance with RO-2 waves cannot provide an effective deceleration. The resonance with RO-1 waves takes place for ions having velocities larger than $1.9 V_A$. So, not many ions can resonate with RO-1 waves. Only resonances with LI-1 waves can provide effective deceleration. The resonances of ions with LO-2 and LI-1 waves may help to form a stable distribution.

[25] This conclusion is corroborated by a 2-D simulation of the time-dependent diffusion process, with the assumption that there is enough wave energy in these wave fields, whereby simultaneous diffusion in both wave fields is avoided. The initial velocity distribution was assumed to be a Maxwellian distribution with $w_{\parallel} = w_{\perp} = 10$ km/s and $u_{\parallel} = 65$ km/s. The computational grid spanned a range in v_{\parallel} from 25 km/s to 105 km/s, and in v_{\perp} from 0 km/s to 60 km/s, with a grid size of 1 km/s for both components. The time step was chosen to be 3×10^{-4} s. The parameters for the outward second-branch LHP waves LO-2 were: $\eta = 1$, $k_0 = 10^{-10}/\text{cm}$ and $P_0 = 6.8 \times 10^{-3} \text{ G}^2\text{cm}$; for the inward first-branch LHP waves LI-1: $\eta = 5/3$, $k_0 = 10^{-10}/\text{cm}$ and $P_0 = 1.36 \times 10^{-1} \text{ G}^2\text{cm}$.

[26] As we can infer from Figure 1, O^{6+} ions can resonate in a certain velocity range with both LO-2 as well as LI-1 waves. As pointed out previously [Isenberg, 2001b], the cross plateau diffusion resulting from interactions with the two wave modes is an important process in the formation and evolution of O^{6+} velocity distribution. To show the full evolution of the ion velocity distribution, and to consider this cross-plateau diffusion, may be a future task but is not the aim of the present paper. The present simulation just intends to show that the acceleration caused by LO-2 waves and deceleration by LI-1 waves can together generate a stable O^{6+} distribution, with a bulk drift velocity that is approximately consistent with the observations.

[27] As a first step to demonstrate the possibility of this new idea, we assume for simplicity that in the simulation those ions with a parallel velocity less than a critical velocity, of say 54 km/s, are in resonance only with LO-2 waves, while ions having larger parallel velocities are in resonance only with LI-1 waves. We also assume that the phase space densities are continued across the vertical line

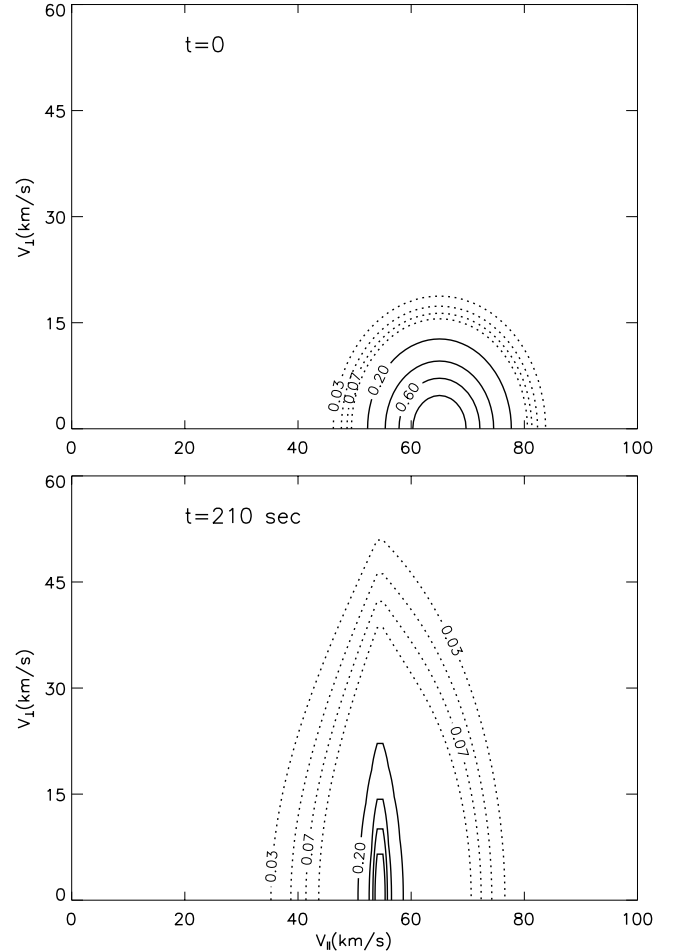


Figure 6. The evolution of the velocity distribution of O^{6+} ions is controlled by diffusion driven by resonance with waves of the LI-1 and LO-2 branch. The upper panel shows the initially assumed bi-Maxwellian distribution with $w_{\parallel} = w_{\perp} = 10$ km/s and $u_{\parallel} = 65$ km/s. The bottom panel shows the simulation results after 700001 time steps in the numerical calculation, corresponding to 210 s. A time step is 3×10^{-4} s.

with $v_{\parallel} = 54$ km/s and determined from the parallel diffusion flux on both sides, by considering the density conservation law.

[28] Figure 6 shows the simulation results. The upper panel shows the initial unstable distribution function, and the bottom panel the resulting final stable distribution. The final bulk velocity is 55.8 km/s, the anisotropy $A = (T_{\perp}/T_{\parallel} - 1)$ is 4.33, and the parallel and perpendicular thermal velocities are, respectively, 12.6 km/s and 29 km/s. With these parameters our model may explain qualitatively the observational result presented by *Hefti et al.* [1998].

[29] In the above simulation we assumed that there is enough wave energy in the LO-2 mode. We will show that, if the LO-2 wave intensity is zero, the Oxygen ions may still keep a high drift speed. In Figure 7 the numerical results are shown, which were obtained from the integration of the diffusion equation, whereby the diffusion coefficient is determined solely by LI-1 waves. The left boundary of the diffusion domain is at $v_{\parallel} = 30.6$ km/s, equal to $1.02V_A$, at

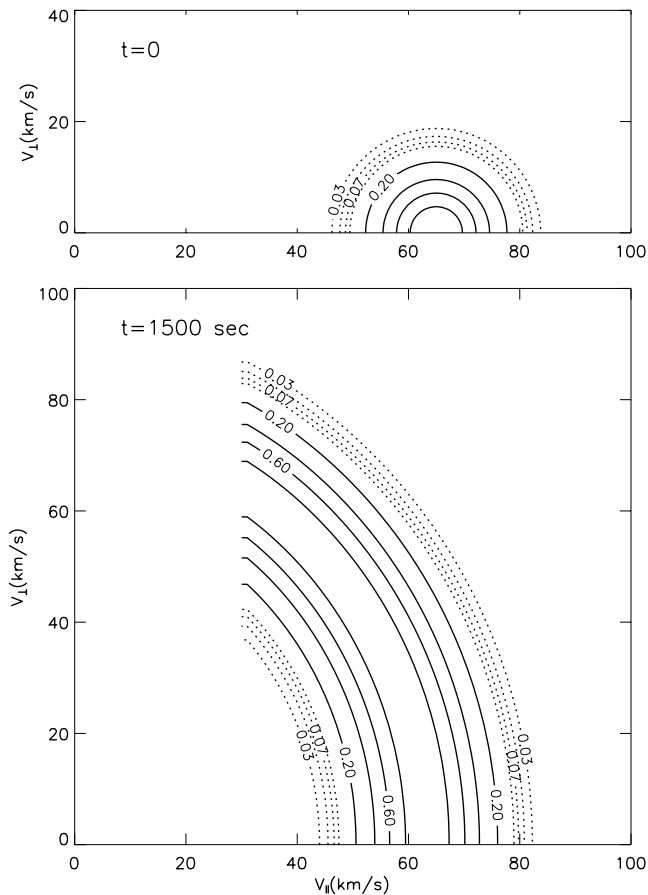


Figure 7. The evolution of velocity distribution of O^{6+} ions is controlled by diffusion caused solely by waves of the LI-1 branch. The format is the same as Figure 6.

which the resonant line of O^{6+} detaches from the LI-1 dispersion curve. The boundary conditions are, a constant extrapolation at $v_{\perp} = 0$ and $v_{\parallel} = 30.6$ km/s, which guarantees that no ions diffuse across these two boundaries. We see that a stable distribution can be generated through cyclotron-resonance diffusion caused by only LI-1 waves. The resulting bulk velocity is larger than V_A . Its precise value is determined by the initial distribution. In this case it is 47 km/s. The thermal anisotropy of this distribution is fairly high, $A = 9.3$. A detailed future comparison between model calculations and in situ observations will put more constraints on this diffusion model.

[30] It should be pointed out that the bulk speeds of the initial distributions of the Fe^{9+} and O^{6+} ions are different in 4, 6, and 7. The primary purpose of our simulations was to show first that the relevant wave modes can lead to stable (trapped by the waves) velocity distributions (given reasonable boundary conditions). But more importantly, in the discussion of Figure 5 we have pointed out that for O^{6+} ions the LO-1 and LI-1 waves cannot sustain a stable distribution, because of the large gap in the resonant v_{\parallel} range of the O^{6+} ions. Therefore, they got a high drift speed basically owing to their higher charge-per-mass ratio and different wave-resonance condition resulting thereof.

[31] No attempt was made here to find out whether differential speeds can be generated, when one starts with

the same distribution (bulk speed) for both species. Certainly, such a study exploiting our present ideas should be carried out as the next step in the future.

5. Discussion and Conclusion

[32] We have described in this paper a possible novel way of understanding the minor ion drifts, with Fe^{9+} slightly lagging behind O^{6+} , as observed in the solar wind by CELIAS on SOHO [Hefti *et al.*, 1998]. By simply assuming enough wave power to exist on the relevant wave branches considered here, we calculated the plateaus which result from quasi-linear diffusion in resonance of the minor ions with various waves modes, having a dispersion as defined for a cold plasma. A two-dimensional simulation was performed for the purpose of studying the time evolution of ion velocity distributions under the influence of resonances with different types of waves. The different charge-per-mass ratios of the two ion species investigated yield different cyclotron-resonance properties.

[33] The results obtained show that the resonance of Fe^{9+} ions with inward and outward LHP waves on the first dispersion branch can generate and support a stable distribution. It has a bulk velocity very close to the proton bulk velocity. The resonance of O^{6+} oxygen ions with the first branch of inward LHP waves and second branch of outward LHP waves may also lead to the formation of a stable velocity distribution, but with a bulk velocity that is higher than the proton velocity by 56 km/s (differential speed directed along the magnetic field direction). These results are qualitatively consistent with the in situ observations by Hefti *et al.* [1998]. The simulation also shows that even without the second branch of outward LHP waves the O^{6+} ions may, by resonance with only the first branch of inward LHP waves, keep a stable drift velocity higher than V_A .

[34] The observations made of silicon Si^{7+} ions might be explained in the same way as above. Since these ions have a charge-per-mass number of 0.25, they may resonate with both the outward and inward first-branch LHP, and they may thus keep a drift velocity which is lower than that of oxygen. More careful work should be done in the future to understand the drift velocity of silicon ions.

[35] The above calculations are based on assuming the existence of waves with the cold plasma dispersion relation. The results just show a new possibility or way for understanding the differential speed of heavier ions observed in the solar wind by CELIAS on SOHO and only represent a first step towards a particle simulation and self-consistent model, which certainly needs to be developed in the future. To obtain a better understanding of this phenomenon, additional work should be done on other minor ions as well as on the waves.

[36] We do not have at the present time any direct evidence showing the existence of waves obeying the dispersion branches invoked in this paper. Furthermore, the cold plasma dispersion relation may need to be corrected by thermal effects or even evaluated self-consistently, together with the evolving distributions of protons and minor ions. For example, the second branch waves are heavily damped in resonance with ions having a drifting bi-Maxwellian velocity distribution. However, if the shape of the distribution is under intense wave action allowed to

develop resonant plateaus, then absorption will perhaps become much weaker and the waves can exist. We have only considered resonance with a single wave mode in a given speed range, however, simultaneous resonances with two modes may occur. Second-order Fermi acceleration [see, e.g., Isenberg, 2001b] might then become important in this problem too and should be studied in the future.

[37] **Acknowledgments.** The authors thank Prof. K. Sauer for helpful discussions about the thermal plasma dispersion relation and advice concerning its numerical solutions. Tu's and Wang's work was supported by the National Natural Science Foundation of China under projects with contract numbers 40174045 and 49990452, and by the foundation of Major Projects of National Basic Research under contract number G-2000078405.

[38] Shadia Rifai Habbal thanks Adolfo F. Vinas and another referee for their assistance in evaluating this paper.

References

- Bochsler, P., Velocity and abundance of silicon ions in the solar wind, *J. Geophys. Res.*, *94*, 2365–2373, 1989.
- Cranmer, S., Ion cyclotron diffusion of velocity distributions in the extended solar corona, *J. Geophys. Res.*, *106*, 24,937–24,954, 2001.
- Davidson, R. C., *Methods in Nonlinear Plasma Theory*, Academic, San Diego, Calif., 1972.
- Denskat, K. U., and F. M. Neubauer, Statistical properties of low-frequency magnetic field fluctuations in the solar wind from 0.29 to 1.0 AU during solar minimum conditions: HELIOS 1 and HELIOS 2, *J. Geophys. Res.*, *87*, 2215, 1982.
- Gendrin, R., Pitch angle diffusion of low energy protons due to gyro-resonant interaction with hydromagnetic waves, *J. Atmos. Terres. Phys.*, *30*, 1313–1330, 1968.
- Gendrin, R., and A. Roux, Energization of helium ions by proton-induced hydromagnetic waves, *J. Geophys. Res.*, *85*, 4577–4586, 1980.
- Gomberoff, L., and H. Astudillo, Ion heating and acceleration in the solar wind, in *Solar Wind Nine*, edited by S. R. Habbal et al., pp. 461–464, Am. Inst. of Phys., Melville, N.Y., 1999.
- Gomberoff, L., and R. Elgueta, Resonant acceleration of alpha particles by ion-cyclotron waves in the solar wind, *J. Geophys. Res.*, *96*, 9801–9804, 1991.
- Gomberoff, L., F. T. Gratton, and G. Gnani, Acceleration and heating of heavy ions in high speed solar wind streams, in *Solar Wind Eight*, edited by D. Winterhalter et al., 319 pp., Am. Inst. of Phys., Melville, N.Y., 1996a.
- Gomberoff, L., F. T. Gratton, and G. Gnani, Acceleration and heating of heavy ions by circularly polarized Alfvén waves, *J. Geophys. Res.*, *101*, 15,661–15,665, 1996b.
- Hefti, S., et al., Kinetic properties of solar wind minor ions and protons measured with SOHO/CELIAS, *J. Geophys. Res.*, *103*, 29,697–29,704, 1998.
- Hollweg, J. V., The cyclotron resonance in coronal holes: 2. A two-proton description, *J. Geophys. Res.*, *104*, 24,793, 1999a.
- Hollweg, J. V., The cyclotron resonance: Heating of protons and oxygen in coronal holes, in *Solar Wind Nine*, edited by S. R. Habbal et al., 369 pp., Am. Inst. of Phys., Melville, N. Y., 1999b.
- Hollweg, J. V., The cyclotron resonance in coronal holes: 1. Heating and acceleration of protons, O^{+5} , and Mg^{+9} , *J. Geophys. Res.*, *104*, 24,781, 1999c.
- Hollweg, J. V., The cyclotron resonance in coronal holes: 3. A five-beam turbulence-driven model, *J. Geophys. Res.*, *105*, 15,699, 2000.
- Hu, Y.-Q., A four-fluid turbulence-driven solar wind model for preferential acceleration and heating of heavy ions, *J. Geophys. Res.*, *105*, 5093–5111, 2000.
- Isenberg, P. A., Resonant acceleration and heating of solar wind ions: Anisotropy and dispersion, *J. Geophys. Res.*, *89*, 2133, 1984.
- Isenberg, P. A., Heating of coronal holes and generation of the solar wind by ion-cyclotron resonance, *Space Sci. Rev.*, *95*, 119–131, 2001a.
- Isenberg, P. A., The kinetic shell model of coronal heating and acceleration by ion cyclotron waves: 2. Inward and outward propagating waves, *J. Geophys. Res.*, *106*, 29,249–29,260, 2001b.
- Isenberg, P. A., and J. V. Hollweg, On the preferential acceleration and heating of solar wind heavy ions, *J. Geophys. Res.*, *88*, 3923–3935, 1983.
- Isenberg, P. A., and M. A. Lee, A dispersive analysis of bi-spherical pickup ion distribution, *J. Geophys. Res.*, *101*, 11,055–11,066, 1996.
- Isenberg, P. A., M. A. Lee, and J. V. Hollweg, A kinetic model of coronal heating and acceleration by ion-cyclotron waves: Preliminary results, *Sol. Phys.*, *193*, 247–257, 2000.
- Isenberg, P. A., M. A. Lee, and J. V. Hollweg, The kinetic shell model of coronal heating and acceleration by ion-cyclotron waves: 1. Outward-propagating waves, *J. Geophys. Res.*, *106*, 5649–5660, 2001.
- Kennel, C. F., and F. Engelmann, Velocity space diffusion from weak plasma turbulence in a magnetic field, *Phys. Fluids*, *9*, 2377–2388, 1966.
- Marsch, E., Dissipation and wave-ion interaction in the solar wind: Links between fluid and kinetic theory, *Nonlinear Proc. Geophys.*, *6*, 149–160, 1999.
- Marsch, E., and C.-Y. Tu, Evidence for pitch-angle diffusion of solar wind protons in resonance with cyclotron waves, *J. Geophys. Res.*, *106*, 8357–8361, 2001.
- Marsch, E., K.-H. Mühlhauser, R. Schwenn, H. Rosenbauer, W. Pilipp, and F. M. Neubauer, Solar wind protons: Three-dimensional velocity distributions and derived plasma parameters measured between 0.3 and 1 AU, *J. Geophys. Res.*, *87*, 52–72, 1982a.
- Marsch, E., K.-H. Mühlhauser, H. Rosenbauer, R. Schwenn, and F. M. Neubauer, Solar wind helium ions: Observations of the Helios solar probes between 0.3 and 1 AU, *J. Geophys. Res.*, *87*, 35–51, 1982b.
- Marsch, E., C. K. Goertz, and K. Richter, Wave heating and acceleration of solar wind ions by cyclotron resonance, *J. Geophys. Res.*, *87*, 5030–5044, 1982c.
- Neugebauer, M., The solar-wind and heliospheric magnetic field in three dimensions, in *The Heliosphere Near Solar Minimum*, edited by A. Balogh et al., pp. 43–106, Springer-Verlag, New York, 2001.
- Ofman, L., A. Vinas, and S. P. Gary, Constraints on the O^{5+} anisotropy in the solar corona, *Astrophys. J.*, *547*, L175–L178, 2001.
- Rowlands, J., V. D. Shapiro, and V. I. Shevchenko, Quasilinear theory of plasma cyclotron instability, *Sov. Phys. JETP, Engl. Trans.*, *23*, 651–660, 1966.
- Schmid, J., P. Bochsler, and J. Geiss, Velocity of iron ions in the solar wind, *J. Geophys. Res.*, *92*, 9901–9906, 1987.
- Shapiro, V. D., and V. I. Shevchenko, The nonlinear theory of interaction between charged particle beams and a plasma in a magnetic field, *Sov. Phys. JETP, Engl. Transl.*, *15*, 1053–1061, 1962.
- Skilling, J., Cosmic rays in the galaxy: Convection or diffusion?, *Astrophys. J.*, *170*, 265–273, 1971.
- Stix, T. H., *Waves in Plasmas*, Am. Inst. of Phys., Melville, N. Y., 1992.
- Tam, S. W. Y., and T. Chang, Kinetic evolution and acceleration of the solar wind, *Geophys. Res. Lett.*, *26*, 3189–3192, 1999.
- Tam, S. W. Y., and T. Chang, Effect of electron resonant heating on the kinetic evolution and acceleration of the solar wind, *Geophys. Res. Lett.*, *28*, 1351–1354, 2001.
- Tu, C.-Y., and E. Marsch, On cyclotron wave heating and acceleration of solar wind ions in the outer corona, *J. Geophys. Res.*, *106*, 8233–8252, 2001a.
- Tu, C.-Y., and E. Marsch, Wave dissipation by ion cyclotron resonance in the solar corona, *Astron. Astrophys.*, *368*, 1071–1076, 2001b.
- Tu, C.-Y., and E. Marsch, Anisotropy regulation and plateau formation through pitch angle diffusion of solar wind protons in resonance with cyclotron waves, *J. Geophys. Res.*, *107*(A9), 1249, doi:10.1029/2001JA000150, 2002.
- Tu, C.-Y., L.-H. Wang, and E. Marsch, Formation of the proton beam distribution in high-speed solar wind, *J. Geophys. Res.*, *107*(A10), 1291, doi:10.1029/2002JA009264, 2002.
- Tu, C.-Y., E. Marsch, and L.-H. Wang, Cyclotron-resonant diffusion regulating the core and beam of the solar wind proton distributions, in *Solar Wind 10*, Am. Inst. of Phys., Melville, N.Y., in press, 2003.
- Vocks, C., and E. Marsch, Kinetic results for ions in the solar corona with wave-particle interactions and Coulomb collisions, *Astrophys. J.*, *568*, 1030–1042, 2002.

E. Marsch, Max-Planck-Institut für Aeronomie, Max-Planck-Str. 2, D-37191 Katlenburg-Lindau, Germany. (marsch@linmpi.mpg.de)

C.-Y. Tu, Department of Geophysics, Center for Space Science, Peking University, CAS, Beijing 100871, China. (cytu@public3.bta.net.cn)

L.-H. Wang, Department of Physics and Space Science Laboratory 7450, University of California, Berkeley, CA 94720-7450, USA. (wanglh@uclink.berkeley.edu)